

## **General Disclaimer**

### **One or more of the Following Statements may affect this Document**

- This document has been reproduced from the best copy furnished by the organizational source. It is being released in the interest of making available as much information as possible.
- This document may contain data, which exceeds the sheet parameters. It was furnished in this condition by the organizational source and is the best copy available.
- This document may contain tone-on-tone or color graphs, charts and/or pictures, which have been reproduced in black and white.
- This document is paginated as submitted by the original source.
- Portions of this document are not fully legible due to the historical nature of some of the material. However, it is the best reproduction available from the original submission.

# Influence of Composition on the Microstructure and Mechanical Properties of a Nickel-Base Superalloy Single Crystal

(NASA-TM-83563) INFLUENCE OF COMPOSITION ON  
THE MICROSTRUCTURE AND MECHANICAL PROPERTIES  
OF A NICKEL-BASE SUPERALLOY SINGLE CRYSTAL  
(NASA) 11 p HC A02/MF A01 CSCL 11F

N84-17354

Unclas  
G3/26 18413

Michael V. Nathal  
*Lewis Research Center*  
*Cleveland, Ohio*

and

Lynn J. Ebert  
*Case Western Reserve University*  
*Cleveland, Ohio*



Prepared for the  
Fifth International Symposium on Superalloys  
sponsored by the American Institute of Mining,  
Metallurgical and Petroleum Engineers  
Seven Springs, Pennsylvania, October 7-11, 1984

**NASA**

INFLUENCE OF COMPOSITION OF THE MICROSTRUCTURE AND MECHANICAL PROPERTIES  
OF A NICKEL-BASE SUPERALLOY SINGLE CRYSTAL

Michael V. Nathal  
National Aeronautics and Space Administration  
Lewis Research Center  
Cleveland, Ohio 44135 U.S.A.

and

Lynn J. Ebert  
Case Western Reserve University  
Department of Metallurgy and Materials Science  
Cleveland, Ohio 44106 U.S.A.

Summary

The effects of cobalt, tantalum, and tungsten contents on the microstructure and mechanical properties of single crystal Mar-M247 were investigated. Elevated temperature tensile and creep-rupture properties of [001] oriented single crystals were related to microstructural features of the alloys. Substitution of Ni for Co in the high refractory metal alloys increased the lattice mismatch, which was considered to be the cause of the increases in tensile and creep strength. Substitution of Ni for Ta caused large decreases in tensile strength and creep life, consistent with decreases in  $\gamma'$  volume fraction, lattice mismatch, and solid solution hardening. Substitution of W for Ta resulted in decreased life at high stresses, which was related to small decreases in mismatch and volume fraction. However, the W substitution resulted in improved life at low stresses, which was related to solid solution strengthening by W.

## Introduction

The introduction of single crystals has resulted in significant improvements in the creep resistance of nickel-base superalloys. It is well known that this is primarily the result of removal of the grain boundary strengthening elements C, B, Zr, and Hf. This compositional modification increases the incipient melting temperature such that coarse as-cast  $\gamma'$  structures can be completely dissolved during heat treatment and subsequently re-precipitated as a fine dispersion (1,2). The removal of grain boundary elements also changes the roles of the other elements in an alloy. For example, in polycrystalline Mar-M247, reduction of Co level from 10 to 0 percent caused a reduction in creep life (3), whereas comparison of two alloys in a study on single crystals (2) indicated that removal of Co actually increased life. An explanation for the difference in the role of Co in the polycrystalline and single crystal materials lies in the absence of the grain boundary elements in the single crystal version. In polycrystalline Mar-M247, Ta is present mostly in the MC carbides, whereas in the single crystal alloy, C is absent and Ta is free to partition between the  $\gamma$  and  $\gamma'$  phases. However, the influence of Ta and its interaction with Co have not been previously investigated.

The purpose of this investigation was to examine the influence of Co, Ta, and W on the microstructure and mechanical properties of single crystal Mar-M247. Cobalt and Ta are considered strategic (4), and thus there is motivation for conservation of these materials. In addition, these elements could provide useful insight on factors controlling the creep resistance of single crystals. Accordingly, a matrix of alloy compositions was designed and is presented in Table I. Alloy G, which contains 10 percent Co, 3 percent Ta, and 10 percent W, is the standard version of Mar-M247 stripped of C, B, Zr, and Hf. At the baseline 3Ta-10W refractory metal level, Ni was substituted for Co to form Alloy E with 5 percent Co and Alloy B with 0 percent Co. Ni was substituted for Ta at each Co level, which produced Alloys A, D, and F. Substitution of W for Ta at 0 and 10 percent Co produced Alloys C and H, respectively. Tungsten was chosen as a substitute because it is close to Ta in the periodic table, it is known to partition to  $\gamma'$  in some alloys, and it is not considered a strategic element. It should be noted that Alloy B is also known as NASAIR 100 (2), and that Alloy E is very close to Alloy 3 in (2).

TABLE I  
Composition of Single Crystal Alloys (Wt. Percent)

	A	B	C	D	E	F	G	H
Ni	74.3	69.7	72.3	69.7	66.4	64.7	61.7	62.5
Co	0	0	0	5.2	5.0	10.1	10.1	10.1
Ta	0	2.82	0	0	2.98	0	2.8	0
W	9.2	10.2	11.8	9.0	9.9	9.0	9.7	11.7
Al	5.2	5.7	5.3	5.2	5.2	5.3	5.2	5.3
Cr	9.2	9.2	8.6	8.8	8.5	8.9	8.5	8.6
Ti	1.4	1.5	1.4	1.4	1.4	1.4	1.4	1.2
Mo	0.7	1.0	0.6	0.7	0.6	0.7	0.6	0.7
C	0.002	0.005	0.005	0.003	0.004	0.004	0.006	0.002
O*	32	20	37	27	33	30	37	50
N*	3	4	3	3	5	3	4	4
B	0.001	0.003	0.005	0.001	0.002	0.001	0.001	0.001
Zr	<0.01	<0.01	<0.01	<0.01	<0.01	<0.01	<0.01	<0.01

Note: \* ppm

A total of nine single crystal castings was produced by the withdrawal process, one each for the eight compositions, plus one additional casting of Alloy B. Note that the actual W concentrations given in Table I for Alloys A, D, and F, which were intended to be 10 percent, were about one weight percent low. Similarly, Alloys C and H actually contained 12 percent W rather than the intended 13 percent. All alloys were given a solution treatment of  $1302 \pm 3^\circ\text{C}$  for 4 hours, followed by forced air quenching. A simulated coating cycle of  $982^\circ\text{C}$  for 5 hours, and a final age of  $871^\circ\text{C}$  for 20 hours completed the heat treatments. Crystals with orientations within  $10^\circ$  of  $[001]$  were utilized for mechanical testing. Tensile tests at an initial strain rate of  $2.2 \times 10^{-4} \text{ sec}^{-1}$ , and constant load creep tests were performed in air at  $1000^\circ\text{C}$ . Mechanical tests were performed on specimens with a 20 mm gage length and a 4.6 mm diameter. X-ray diffraction using  $\text{Cu K}\alpha$  radiation on oriented single crystal disks was used to measure the lattice mismatch between  $\gamma$  and  $\gamma'$ .

### Results and Discussion

#### Microstructure

A high volume fraction of fine cubic or spherical  $\gamma'$  precipitates, approximately  $0.25 \mu\text{m}$  in size, was present in all alloys. Figure 1 illustrates the fully heat treated microstructures of selected single crystal alloys. The morphology of the  $\gamma'$  particles was related to the lattice mismatch  $\delta$ , where  $\delta$  is defined by Equation 1 and  $A_{\gamma'}$  and  $A_\gamma$  are the lattice parameters of the two phases:

$$\delta = 2 (A_{\gamma'} - A_\gamma) / (A_{\gamma'} + A_\gamma) \quad [1]$$

Alloy B exhibited cubic  $\gamma'$  particles, which is indicative of a relatively large lattice mismatch, Figure 1a. Substitution of Ni for Ta in Alloy B to form Alloy A caused a reduction in mismatch and a change to spherical  $\gamma'$ , Figure 1b, as did the addition of 10 percent Co to form Alloy G, Figure 1c. Alloy B, with 0 percent Co and the baseline 3Ta-10W refractory metal level, possessed the largest magnitude of lattice mismatch, exhibiting  $\delta = -0.0035$  at  $25^\circ\text{C}$ . Substitution of W for Ta to form Alloy C reduced  $\delta$

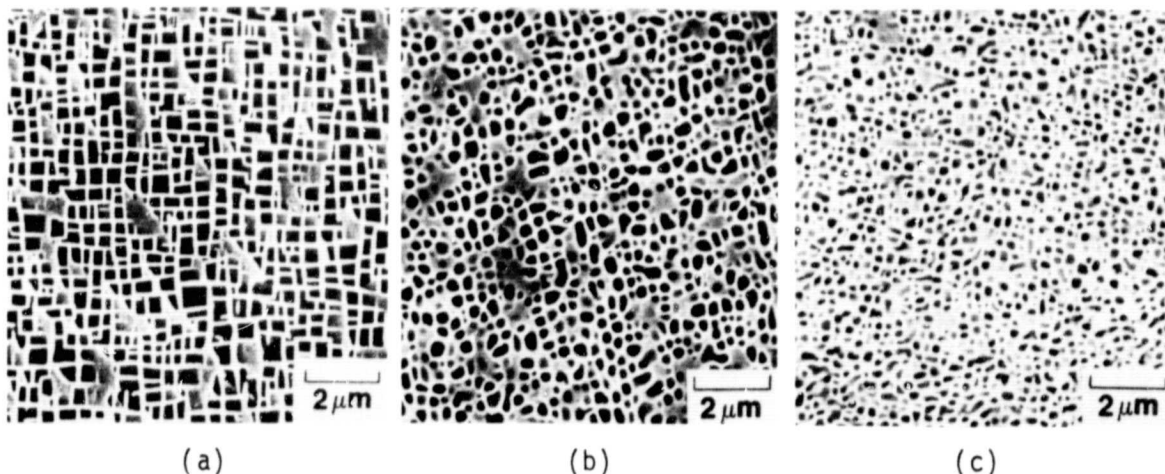


Figure 1. Scanning electron micrographs of fully heat treated single crystal alloys: (a) Alloy B, (b) Alloy A, (c) Alloy G.

to  $-0.002$ , whereas substitution of Ni for Ta to form Alloy A caused a reduction in mismatch to below the detection limit. Similarly, all alloys with 5 and 10 percent Co exhibited  $\delta$  values too small to measure by X-ray diffraction.

The volume fraction of  $\gamma'$  was measured by quantitative metallography on failed creep-rupture specimens. After creep-rupture testing, the cubic or spherical  $\gamma'$  particles coarsened into lamellae perpendicular to the applied stress. The uniform lamellar structure was quite suitable for the use of the line intercept technique for the determination of volume fraction. In addition, most of the  $\gamma'$  that precipitated during cooling from the testing temperature was in the form of fine spherical precipitates, and thus could be distinguished from the lamellar  $\gamma'$ . Therefore, the measurements on creep tested specimens were more representative of the  $\gamma'$  volume fraction at the creep testing temperature of  $1000^{\circ}\text{C}$ . The amount of the strengthening  $\gamma'$  phase is plotted versus Co level in Figure 2. The fraction of  $\gamma'$  was only weakly dependent on Co level, but was strongly dependent on the refractory metal level. The baseline 3Ta-10W alloys had the highest percentages of  $\gamma'$ . Reduction of Ta from the baseline caused decreases in  $\gamma'$  fraction of about 6 volume percent, and substitution of W for Ta resulted in decreases of approximately 2 percent.

In order to determine the relationship of microstructural stability to the creep properties, samples were aged for times of up to 976 hours at  $1000^{\circ}\text{C}$ . Long term thermal exposure can result in precipitation of additional phases,  $\gamma'$  coarsening, and loss of coherency. Only alloys with 0 percent Co and high Ta plus W totals exhibited third phase precipitation. In this alloy system,  $\alpha$ -W and  $\mu$  phases have been observed, and both of these are W-rich. Alloy B exhibited about 0.8 weight percent  $\alpha$ -W in the heat treated condition. After aging for 976 hours, additional  $\alpha$  and  $\mu$  precipitated, totaling approximately 3 percent. Alloy C, which was free of third phases in the heat treated condition, exhibited about 0.5 percent of W-rich phases after 976 hours at  $1000^{\circ}\text{C}$ .

Another aspect of microstructural stability is the Ostwald ripening of the  $\gamma'$  particles. In agreement with previous studies (5,6), a  $t^{1/3}$  time dependence for  $\gamma'$  particle growth was observed. The  $\gamma'$  coarsening rate,  $k$ , was obtained from the slopes of  $(a/2)^3$  versus time, where  $a$  is the average edge length of a  $\gamma'$  cube. Figure 3 illustrates that for most of the alloys, the coarsening rate decreased as Co content increased. Although this effect has been observed previously (6), the reasons for this effect cannot be specified, as it appears that Co additions influence several features that may decrease  $\gamma'$  coarsening. An unexpected result was that refractory metal level did not affect the coarsening rate. It was expected that alloys with higher levels of the slower diffusing Ta and W would have lower coarsening rates, but evidently the magnitudes of the compositional changes were insufficient to cause significant changes in  $\gamma'$  coarsening rates. Alloys B and C, with 0 percent Co and high refractory metal contents, were exceptions to the above trends and exhibited anomalously low coarsening rates. These low rates appear to be related to the higher lattice mismatch in these alloys, which resulted in a loss of coherency during aging. This stabilization against particle coarsening appears to be the result of the reduced mobility of the semi-coherent interface, because motion of the interface would require climb of the hexagonal array of misfit dislocations (7). Also, the loss of coherency involves a reduction in the total energy of the system, which may reduce the driving force for coarsening.

ORIGINAL PAGE IS  
OF POOR QUALITY

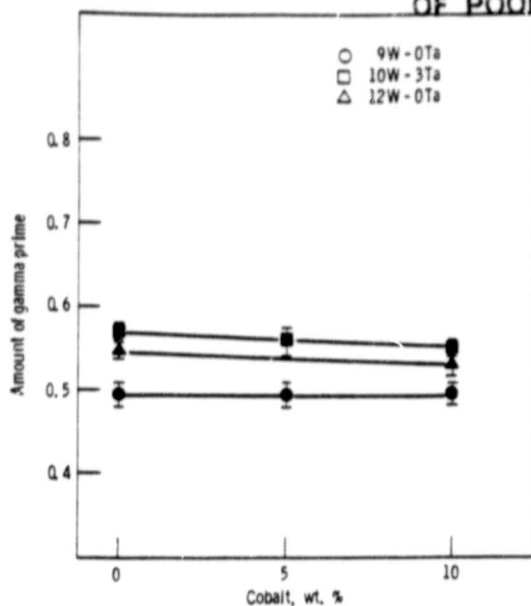


Figure 2. The volume fraction of  $\gamma'$  phase in the single crystal alloys.

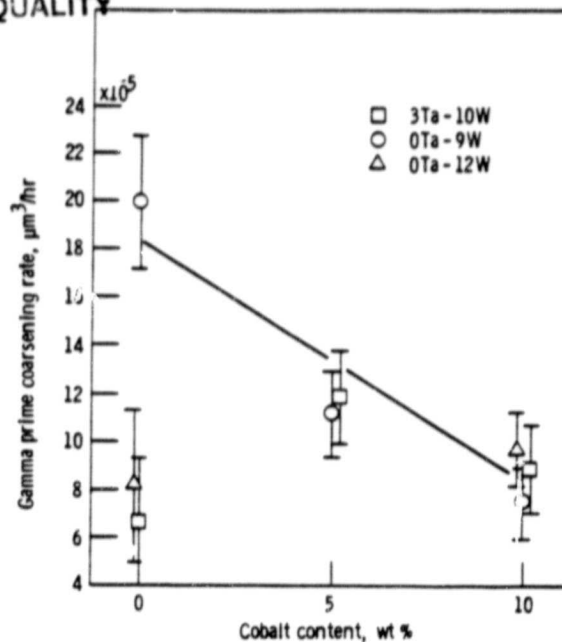


Figure 3. Gamma prime coarsening rates for the single crystal alloys.

All alloys exhibited pronounced, directional  $\gamma'$  coarsening during creep testing at  $1000^{\circ}\text{C}$ . Figure 4 presents the microstructural changes in Alloy B during creep at  $1000^{\circ}\text{C}$  and 148 MPa. After 20 hours into the creep test, the  $\gamma'$  has coalesced into plates perpendicular to the applied stress, as shown in Figure 4a. Although this time was still within the primary creep stage, the  $\gamma'$  platelet structure was already well developed. The average thickness of the plates was measured to be  $0.25\text{ }\mu\text{m}$ , essentially equal to the initial  $\gamma'$  particle size. This structure remains relatively constant throughout the secondary creep stage. For example, after 435 hours, the only noticeable change was a slight thickening of the plates to approximately  $0.33\text{ }\mu\text{m}$ , Figure 4b. After failure at 790 hours, the  $\gamma'$  plates became more irregular and thickened to a value of  $0.77\text{ }\mu\text{m}$ .

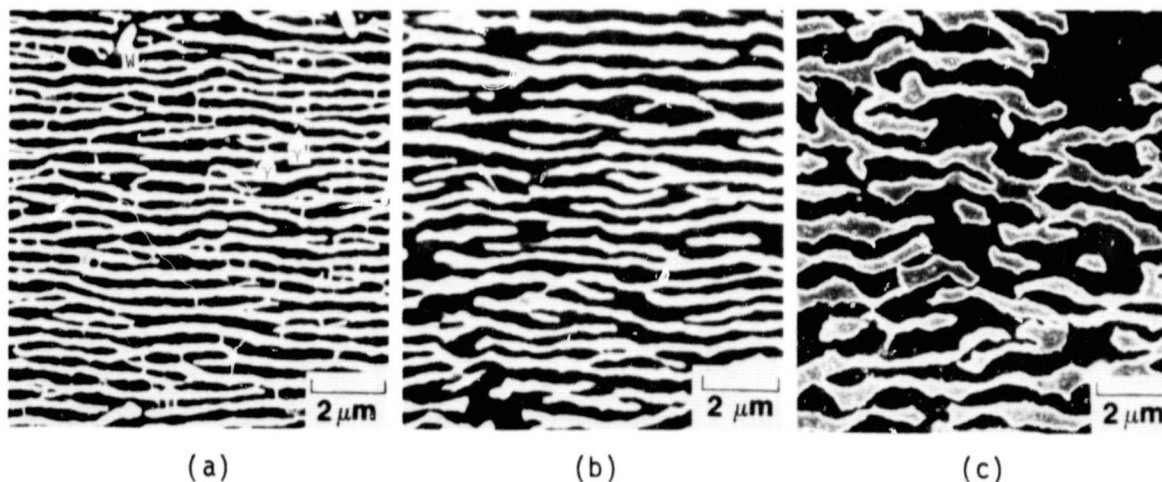


Figure 4. Longitudinal microstructures of Alloy B creep tested at  $1000^{\circ}\text{C}$  and 148 MPa for (a) 20 hours, (b) 434.5 hours, (c) 790 hours.

The 1000°C yield strengths of the single crystal alloys are presented in Figure 5. For the baseline 3Ta-10W alloys, reduction of Co resulted in significant increases in strength. Reduction of Ta from the baseline level caused large decreases in yield strength, and for these alloys, the influence of Co content was largely eliminated. Substitution of W for Ta caused an intermediate reduction in strength, and again the influence of Co was not large. The trends of the ultimate tensile strengths were similar to those of the yield strength data in Figure 4. Additionally, all alloys exhibited tensile elongations of at least 20 percent, and in general the lower strength alloys possessed higher ductilities.

A summary of the creep behavior is presented in Figure 6, where the stress dependence of the steady state creep rate is plotted for each Co level. The actual data for this summary plot are presented elsewhere (8). As shown in Figure 6, the influence of Co on the baseline 3Ta-10W Alloys (B, E, and G) was relatively independent of applied stress, and decreasing Co resulted in improved creep resistance. This figure also indicates that at all applied stresses and Co levels, the OTa-9W Alloys (A, D, and F) were by far the least creep resistant alloys. At a given applied stress, these alloys crept at a rate approximately an order of magnitude faster than the other alloys. However, substitution of W for Ta affected properties differently at different stresses. For example, Alloy B was more creep resistant than Alloy C at high applied stresses. As the stress was decreased, the higher stress dependence of the creep rate of Alloy C resulted in a cross-over in strength such that Alloy C was more creep resistant at low stresses. At a stress of 125 MPa, the creep rate of Alloy B was five times faster than that of Alloy C.

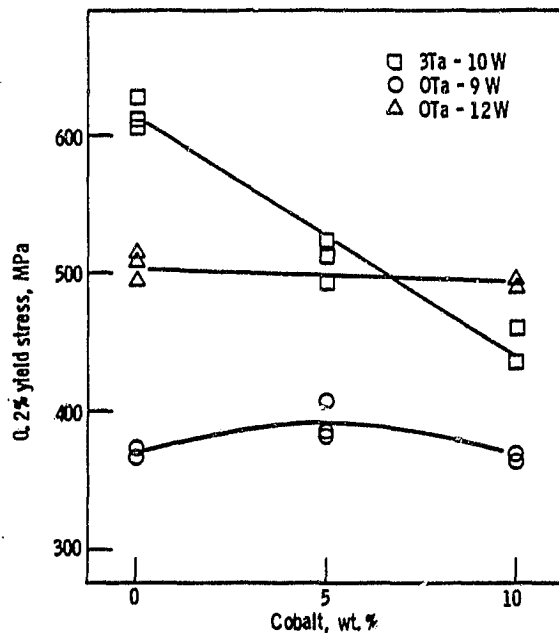


Figure 5. The 0.2 pct yield stress at 1000°C for the single crystal alloys.

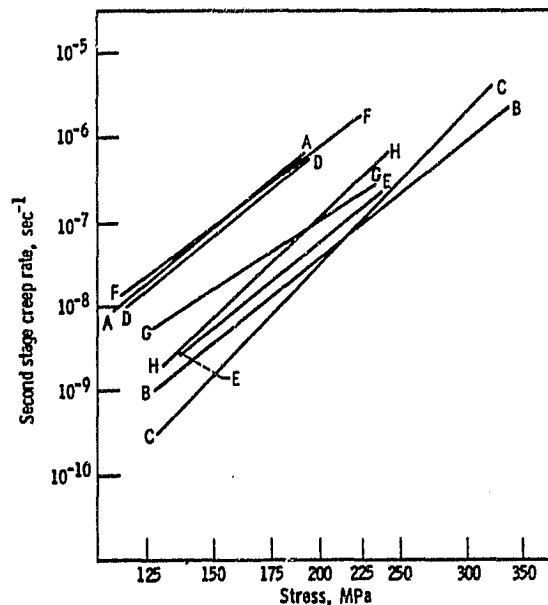


Figure 6. Summary plot of the stress dependence of the steady state creep rates of the single crystal alloys at 1000°C.

## Relationship of Microstructure to Mechanical Behavior

Variations in alloy composition produced some interesting variations in mechanical properties. The reductions in tensile strength as Ni was substituted for Ta was expected, and can be explained by the reductions in  $\gamma'$  volume fraction, solid solution hardening, and mismatch as Ta level was decreased. These arguments are also consistent with the decreases in creep resistance caused by the same alloying changes. The strong influence of Co content on the tensile strength of the 3Ta-10W alloys can be explained by the increased  $\gamma$ - $\gamma'$  mismatch as Co level was reduced. The increased mismatch would increase the contribution of coherency strain hardening to the strength of these alloys. However, this argument may not apply to longer term testing, whereby the effect of microstructural stability may become important. It has been suggested that higher mismatch values may decrease creep life by enhancing  $\gamma'$  coarsening and thus overaging (9). However, in the present study, there was no correlation between the unstressed  $\gamma'$  coarsening rate and the creep resistance of the alloys. For example, it is apparent that reduction of Co in the 0Ta-9W alloys (A, D, and F) decreased the coarsening rate, Figure 3, yet did not influence the creep properties presented in Figure 6. Further, the 10 percent Co alloys (F, G, and H) all exhibited similar  $\gamma'$  coarsening rates, but had significantly different creep strengths.

For the alloys in the present study, high  $\gamma$ - $\gamma'$  mismatch can actually improve creep resistance. Increased mismatch does cause very rapid coarsening, but only in the initial portions of the creep test. The rapid directional coarsening observed in the present study did not cause the typical overaging response whereby dislocation bypassing mechanisms become easier as the particles grow. In contrast, the formation of the lamellae suppresses bypassing mechanisms, and consequently the mobile dislocations must shear through the  $\gamma'$  phase and the  $\gamma$ - $\gamma'$  interface (10,11). Slip in the  $\gamma'$  phase is considered to be more difficult than slip in  $\gamma$ , due to the ordered structure (11). However, the rate-limiting step in the deformation process appears to be shear through the  $\gamma$ - $\gamma'$  interface. The interface is characterized by a stable hexagonal array of misfit dislocations that can act as obstacles to further dislocation motion. Thus, after dislocations have sheared through either phase, they would be held up at the interface, and recovery events would be necessary to nucleate slip through the next lamella. The beneficial effect of high mismatch is derived from the stronger barrier provided by the more finely spaced misfit dislocations. Once formed, however, the lamellae do coarsen slowly during the remainder of the creep life, and this thickening appears to be related to the onset of tertiary creep (12).

The influence of Co on the present alloys supports the postulate that high lattice mismatch is beneficial for creep resistance. The effects of Co cannot be attributed to solid solution hardening by Co, because the Co additions actually decreased the creep strength of the high refractory metal alloys. In addition, the presence of  $\alpha$  and  $\mu$  phases in the stronger 0 percent Co alloys (B and C) reduced the amount of W in solid solution compared to the alloys with 5 and 10 percent Co. Again, this effect would be expected to increase the strength of the high Co alloys if it would have any effect at all. Although Co content did not influence the strength of the individual phases, it did influence the strength of the  $\gamma$ - $\gamma'$  interface. As Co level was decreased from 5 to 0 percent, the room temperature lattice mismatch increased in magnitude from below the detectability limit to  $\sim 0.0035$ . This increase in mismatch would decrease the spacing of the hexagonal misfit dislocation array, and therefore strengthen the lower Co alloys.

The influence of the substitution of W for Ta on the creep properties was more puzzling. For example, Alloy C had a slightly lower  $\gamma'$  volume fraction and  $\gamma$ - $\gamma'$  mismatch than Alloy B, both of which would be expected to weaken Alloy C in comparison to Alloy B. In fact, these features may explain the results of the short term tests, where Alloy B was indeed stronger. However, some other microstructural feature must cause the observed cross-over in creep resistance at lower applied stresses. One could argue that Alloy C exhibited better creep strength at low stresses because it possessed smaller amounts of W-rich phases than Alloy B. However, this could not explain the same trends in strength at the 10 percent Co level, where both Alloys G and H were free of any third phases. In fact, all present evidence appears to indicate that the precipitation of W-rich phases does not significantly affect the creep resistance of this series of alloys. One possible explanation for the cross-over in creep strength is that W is more effective as a solid solution hardener than Ta. Unfortunately, only limited data are available on the influence of alloying on the various mechanisms by which a solute atom may improve creep resistance. Thus, a possible explanation for the cross-over in strength exhibited between the 0Ta-12W and 3Ta-10W alloys is provided. At high applied stresses, the slight decreases in  $\gamma'$  volume fraction and mismatch cause the 0Ta-12W alloys to be less resistant to plastic flow. At progressively lower stresses, solid solution strengthening becomes more important, which results in the cross-over in creep strength. However, it is recognized that further study is necessary to establish the influence of refractory metals on the creep properties of superalloys.

### Conclusions

The creep behavior of the single crystal alloys was significantly influenced by the  $\gamma'$  morphology which developed during creep. At 1000°C, the  $\gamma'$  particles rapidly coalesced into lamellae perpendicular to the applied stress. This lamellar structure forced the mobile dislocations to shear through the  $\gamma'$  phase and the  $\gamma$ - $\gamma'$  interface. A hexagonal array of misfit dislocations was present at the interface, and acted as a barrier to dislocation motion. Decreases in Co level from 10 to 0 percent caused significant increases in tensile strength and creep resistance for the alloys with high refractory metal levels. These decreases in Co concentration increased the  $\gamma$ - $\gamma'$  mismatch, which resulted in either increased coherency strains during tensile testing, or a finer misfit dislocation spacing during creep testing, both of which provided a stronger obstacle to dislocation flow. Substitution of Ni for Ta caused large reductions in tensile strength and creep resistance, which can be explained by low values of  $\gamma'$  volume fraction, solid solution hardening, and lattice mismatch. Substitution of W for Ta caused decreased creep lives at high stresses, as a result of small decreases in  $\gamma$ - $\gamma'$  mismatch and  $\gamma'$  volume fraction. The W substitution resulted in improved lives at lower stresses, which was believed to be a consequence of the increased effectiveness of W as a solid solution hardener.

## References

1. M. Gell, D. N. Duhl, and A. F. Giamei: Proc. 4th Intl. Symp. on Superalloys, Ed. by J. K. Tien et al., ASM, Metals Park, 1980, p. 205-214.
2. T. E. Strangman, G. S. Hoppin, C. M. Phipps, K. Harris, and R. E. Schwer: Proc. 4th Intl. Symp. on Superalloys, Ed. by J. K. Tien et al., ASM, Metals Park, 1980, p. 215-224.
3. M. V. Nathal, R. D. Maier, and L. J. Ebert: Metall. Trans., 1982, Vol. 13A, p.1767-1774.
4. J. Stephens: NASA TM-81617, 1980.
5. E. H. VanDerMolen, J. M. Oblak, and O. H. Kriege: Metall. Trans., 1971, Vol. 2, p. 1627-1633.
6. C. K. L. Davies, P. Nash, and R. N. Stevens: J. Mat. Sci., 1980, Vol. 15, p. 1521-1532.
7. H. I. Aaronson: in Decomposition of Austenite by Diffusional Processes, Ed. by V. F. Zackay and H. I. Aaronson, Interscience Publishers, N. Y., 1960, p. 387-548.
8. M. V. Nathal: Ph. D. Thesis, Case Western Reserve Univ., 1983.
9. R. F. Decker: Steel Strengthening Mechanisms Symp., Climax Molybdenum Co., 1969, p. 147-170.
10. D. D. Pearson, F. D. Lemkey, and B. H. Kear: Proc. 4th Intl. Symp. on Superalloys, Ed. by J. K. Tien et al., ASM, Metals Park, 1980, p. 513-520.
12. D. D. Pearson, B. H. Kear, and F. D. Lemkey: in Creep and Fracture of Engineering Materials and Structures, Ed. by B. Wilshire and D. R. J. Owen, Pineridge Press, Swansea, UK, 1981, p. 213-233.
11. M. V. Nathal and L. J. Ebert: Scripta Metall., 1983, Vol. 17, p. 1151-1154.